

Chapter 5: Development of a processing route for the fabrication of thin hierarchically porous copper self-standing structure using direct ink writing and sintering for electrochemical energy storage application

This chapter is dedicated to the development and validation of a novel processing route designed to fabricate thin, self-standing HP-*Cu* samples through a combination of DIW and sintering techniques. The primary objective is to produce HP-*Cu* structures with a controlled pore size of less than 200 μm , making them suitable for advanced applications such as energy storage systems (EES). A significant emphasis has been placed on achieving this through a systematic approach that optimizes both the ink rheology and the various process parameters critical to the DIW method.

The innovation of this work is underscored by the development, for the first time, of a copper ink formulation with an exceptionally high particle loading exceeding 95 weight percent (*wt%*). This high loading presents unique challenges in terms of material behavior during the fabrication process, necessitating meticulous optimization to ensure the ink exhibits the required flow properties for DIW. To achieve this, a systematic experimental design was implemented, focusing on key process variables such as copper loading, nozzle diameter, printing speed, and layer thickness. Each of these parameters was carefully studied to understand their influence on the final morphology and structural integrity of the fabricated samples.

The study includes a comprehensive morphological characterization of the fabricated HP-*Cu* samples to determine the optimal process parameters which involves detailed analysis of the pore structure, surface finish, and overall geometrical fidelity of the samples. The insights gained from this analysis have been used to fine-tune the process, ensuring the

production of samples that meet the stringent requirements for porosity and mechanical stability.

Furthermore, a proof-of-concept study was conducted to demonstrate the practical applicability of the developed process. This focused specifically on the fabrication of porous *Cu* structures.

5.1 Results and Discussion

5.1.1 Process parameter optimization

The experimental optimization of the process parameters for the fabrication of HP-*Cu* components using DIW was carried out using a systematic L-9 orthogonal array design. This experimental design facilitated the evaluation of multiple process parameters simultaneously while minimizing the number of experimental trials required. The selected parameters included *Cu* loading, nozzle diameter, layer height (expressed as a percentage of the nozzle diameter), and printing speed. These factors were chosen due to their critical influence on the dimensional accuracy and structural quality of the printed components.

Dimensional deviation was selected as the benchmark property for optimizing the process parameters. This decision was based on previous successful applications of dimensional deviation as a metric for evaluating the quality of printed copper components, as reported in earlier studies. Dimensional deviation serves as a reliable indicator of the fidelity of the printed structure to the intended design dimensions, making it an essential parameter for assessing the effectiveness of the DIW process. The complete combinations of the process parameters utilized in the L-9 experimental design are presented in Table 5.1.

Table 5.1 Experimental Matrix Based on Orthogonal Array Design

Sr. no	<i>Cu</i> Loading wt %	Nozzle diameter (<i>d</i>) mm	Layer height (Δh) %	Print speed (<i>v</i>) mm/s	Dimensional deviation
1	93	0.2	60	5	6.24±0.24
2	93	0.4	70	10	5.60±0.26
3	93	0.6	80	15	5.72±0.35
4	95	0.2	70	15	0.84±0.10
5	95	0.4	80	5	2.42±0.08
6	95	0.6	60	10	1.25 ± 0.14
7	97	0.2	80	10	0.25±0.04
8	97	0.4	60	15	0.74±.06
9	97	0.6	70	5	0.64±.04

An analysis of the results presented in Table 5.1 reveals significant insights into the influence of process parameters on the dimensional accuracy of the fabricated *Cu* green parts. For instance, parts printed with a *Cu* loading of 93 weight percent (*wt%*), a nozzle diameter of 0.2 mm, a layer height equivalent to 60% of the nozzle diameter, and a printing speed of 5 mm/s exhibited a notably high value of dimensional deviation. This result indicates that the selected combination of parameters led to challenges in maintaining the geometric precision of the printed structures, potentially due to suboptimal rheological behavior or layer deposition dynamics under these conditions.

In contrast, a different set of process parameters yielded markedly improved results. Specifically, parts printed with a *Cu* loading of 97 *wt%*, a nozzle diameter of 0.2 mm, a layer height set at 80% of the nozzle diameter, and a printing speed of 10 mm/s demonstrated a low value of dimensional deviation. This observation highlights the critical role of higher *Cu* loading in enhancing the stability of the ink during the printing process, coupled with the synergistic effects of an optimized layer height and printing speed in

minimizing dimensional inaccuracies. The findings underscore the profound impact of process parameter variation on the printing characteristics of the *Cu* green parts. The interplay between *Cu* loading, nozzle diameter, layer height, and printing speed directly affects factors such as ink flow, deposition consistency, and interlayer adhesion, which collectively influence the dimensional fidelity of the printed structures.

For determining the optimum values of the process parameters, the “smaller is the better” filter was applied, since the dimensional deviation should be minimum for the optimum value. Thus, the maximum value of the S/N ratio will give the optimized parameters for the printed parts. The response table 5.2 for the S/N ratio provides insight into the relative influence of different printing parameters, Copper Loading, Nozzle Diameter, Layer Height, and Print Speed on the target performance metric, typically dimensional accuracy in a DIW process. The S/N ratio values at different levels indicate the robustness of each factor, with higher (less negative) values suggesting better and more consistent performance.

Table 5.2 Response table for S/N ratio

Level	Copper Loading	Nozzle diameter	Layer height	Print speed
1	-15.3385	-0.7827	-5.0755	-6.5679
2	-2.7000	-6.6749	-3.1910	-1.6203
3	6.1777	-4.4032	-3.5943	-3.6727
Optimized values of the S/N ratio				
Delta	21.5161	5.8992	1.8845	4.9476
Rank	1	2	4	3

Hence, it can be observed from Table 5.2, that the maximum values of the S/N ratio for the copper loading, nozzle diameter, layer height, and print speed were found to be 6.1777, -0.7827, -3.1910, and -1.6203, respectively.

It can also be inferred from Table 5.2, that copper loading has rank 1, which indicates that it has the highest effect on the dimensional deviation. Layer height with a rank of 4, indicates that the dimensional deviation is least affected by it. The order of effect of various parameters on dimensional deviation was found to be *Cu* loading > Nozzle diameter > Print speed > Layer height. Moreover, based on the S/N ratio, the optimum values of process parameters were determined. The optimum values of *Cu* loading, nozzle diameter, layer height, and printing speed were found to be 97 wt%, 0.2 mm, 70% and 10 mm/s, respectively. The main effect plot showcasing the effect of selected process parameters on the output results is shown in Fig. 5.1 and a detailed discussion highlighting the key effects of these parameters is included in the subsequent sections.

5.1.1.1 Effect of *Cu* loading

Cu loading plays a crucial role in the optimization of the DIW process parameters, as it directly influences the ink's rheological behavior and, consequently, the print quality. As illustrated in Fig. 5.1, a clear trend is observed wherein the dimensional deviation of the printed structures significantly decreases as the *Cu* particle loading is increased from 93 wt% to 97 wt%. This notable reduction in dimensional deviation can be primarily attributed to improvements in the rheological properties of the ink at higher solid loadings.

With the increase in *Cu* content, the ink becomes more viscoplastic, enhancing its structural integrity during and after extrusion. The higher particle concentration contributes to better shape retention and minimizes spreading or deformation of the deposited filaments, thereby ensuring greater dimensional accuracy of the printed geometries. To quantitatively assess

this effect, a detailed rheological characterization was conducted on three different *Cu* ink formulations with varying particle loadings, as previously described in previous chapter.

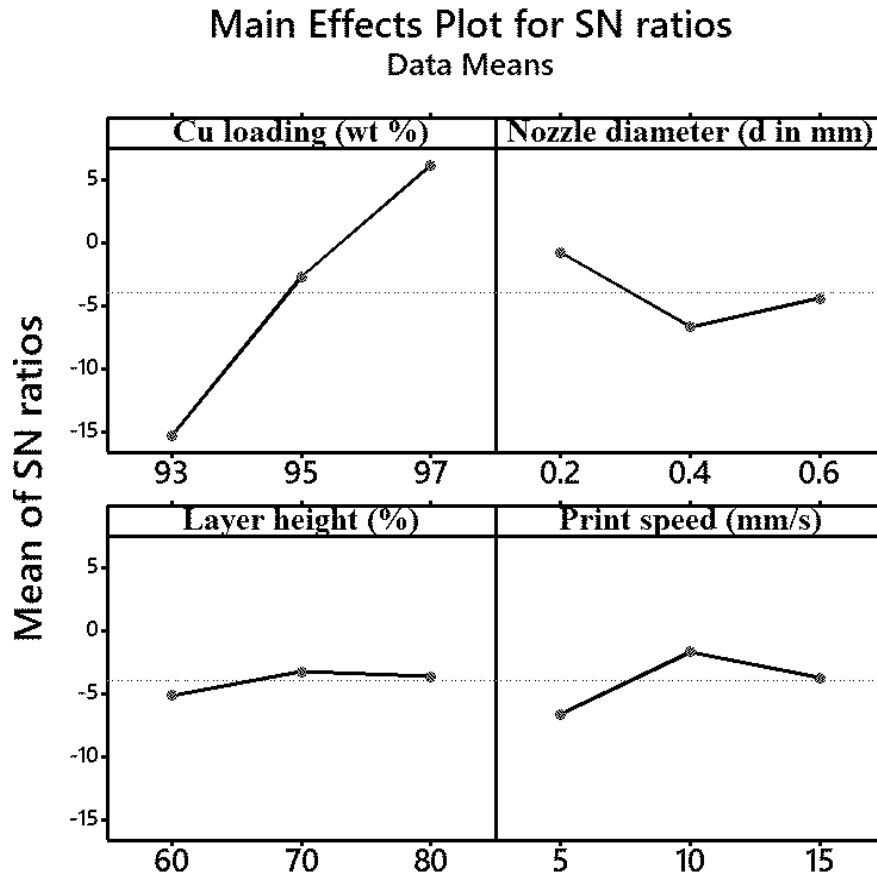


Fig. 5.1: Main effect plots of selected printing parameter

A thorough analysis of the rheological behavior of the developed *Cu* inks revealed significant trends concerning their viscosity and storage modulus, both of which are critical parameters for successful DIW. The developed ink uniformly mixed and wetted by the binder as shown in Fig. 5.2. It was consistently observed that the viscosity of the ink increased with higher particle loading across all examined shear rates. This behavior demonstrates the capability of the ink to maintain its structural integrity and resist deformation during the printing process. Such a characteristic is essential to ensure that the

ink retains its shape when deposited onto the substrate, regardless of the speed of the printing process.

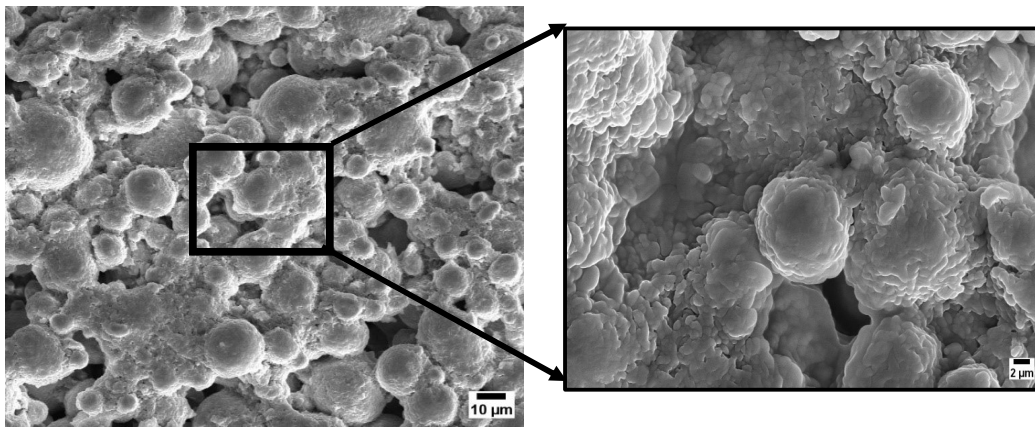


Fig. 5.2 SEM image of prepared ink showing wetting of *Cu* particles

However, a notable reduction in viscosity values was observed as the shear rate increased for all ink formulations. This phenomenon is indicative of the ink's shear-thinning behavior, a desirable property for DIW applications. Shear-thinning ensures that the ink flows smoothly through the nozzle during extrusion while maintaining sufficient viscosity to prevent spreading or sagging once deposited. This dual behavior of the ink i.e. high viscosity at low shear rates for shape retention and reduced viscosity at high shear rates for ease of extrusion highlights its suitability for DIW.

In addition to viscosity, another crucial rheological criterion for successful DIW is the storage modulus of the ink. The storage modulus, which represents the elastic or solid-like behavior of the material, must be sufficiently high to ensure the stability of the printed structure and the prevention of collapse under its weight or during subsequent layer deposition. The relationship between storage modulus and shear rate for three different *Cu* ink formulations was analyzed, and the results are illustrated in previous chapter.

The combination of shear-thinning viscosity behavior and high storage modulus observed in the 97 wt% *Cu* ink underscores its rheological superiority for DIW applications. The ink's ability to flow efficiently through the nozzle at high shear rates while maintaining

robust shape retention and elastic stability at low shear rates ensures its effectiveness in creating high-precision, self-standing structures. These findings further validate the optimization of ink formulation as a critical step in advancing the capabilities of DIW for the fabrication of complex and reliable *Cu* components. Since high storage modulus supports the shape-retaining capacity of the ink after it is extruded, the parts printed with 97 wt % were found to be suitable. Thus, it could be inferred that the *Cu* ink with 97 wt % loading possesses the highest shape-retaining capability. Therefore, owing to the highest values of viscosity and storage modulus, the *Cu* ink with 97 wt % loading exhibited minimum dimensional deviation.

5.1.1.2 Effect of Nozzle diameter & layer height

A detailed analysis of the main effect plot presented in Fig. 5.1 reveals critical insights into the relationship between nozzle diameter and dimensional deviation during the DIW process. The data clearly indicate that the minimum dimensional deviation was achieved when using a nozzle with a diameter of 200 μm . This finding highlights the importance of nozzle size as a key parameter in determining the dimensional accuracy of printed components. As the nozzle diameter was increased from 200 μm to 400 μm , a significant rise in dimensional deviation was observed in the printed structures. This consistent trend indicates that the use of larger nozzle diameters negatively impacts the printing precision and geometric accuracy of the final constructs. One possible explanation for this behavior lies in the direct relationship between nozzle diameter and the thickness of the extruded material. Larger nozzles tend to deposit thicker layers of ink, which can lead to reduced resolution and greater difficulty in maintaining fine structural details. Additionally, with increased layer thickness, the ability to control the shape and placement of each deposited line diminishes, further contributing to dimensional inaccuracies. Therefore, the observed

increase in dimensional deviation with larger nozzle sizes highlights the importance of optimizing nozzle diameter to achieve high-fidelity prints in direct ink writing processes. Specifically, as the nozzle diameter increases, the extruded material forms thicker layers, which can lead to less precise deposition and potential inconsistencies in the layer geometry. Interestingly, a subsequent reduction in dimensional deviation was observed when the nozzle diameter was further increased to 600 μm . This non-linear behavior can be explained by the interplay between nozzle diameter and the formation of layers during the printing process. For instance, at a nozzle diameter of 600 μm , the layer height becomes significantly larger, which results in the formation of curved-shaped layers. This unique layer geometry, while unconventional, may contribute to a reduction in dimensional deviation by providing better interlayer bonding or by mitigating the effects of over-extrusion.

In contrast, for the nozzle diameter of 400 μm , the printed layers were observed to be straight and exhibited no signs of squeezing. This indicates that the 400 μm nozzle diameter produces layers with optimal flatness and uniformity, which might account for the intermediate level of dimensional deviation observed at this nozzle size. The variation in dimensional deviation across different nozzle diameters underscores the complex relationship between nozzle size, layer thickness, and the overall geometry of printed structures. Smaller nozzles, such as the 200 μm diameter, allow for finer precision and greater control over the deposition process, thereby minimizing dimensional inaccuracies. On the other hand, larger nozzles, such as the 600 μm diameter, introduce unique effects related to layer curvature and material flow that can also influence dimensional accuracy. These findings are consistent with prior research, which has highlighted the significant role of nozzle diameter and associated layer thickness in influencing the quality and accuracy of 3D-printed components. The results of this study emphasize the need for a

careful balance in selecting nozzle size to achieve optimal dimensional accuracy, taking into account the interplay between material deposition dynamics and layer geometry. This understanding is crucial for the continued refinement and optimization of DIW processes, particularly for applications requiring high precision and reliability. effect of nozzle diameter and layer height, three samples with a layer height of 60%, 70% and 80% of a constant nozzle diameter were fabricated and the same are shown in Fig. 5.3.

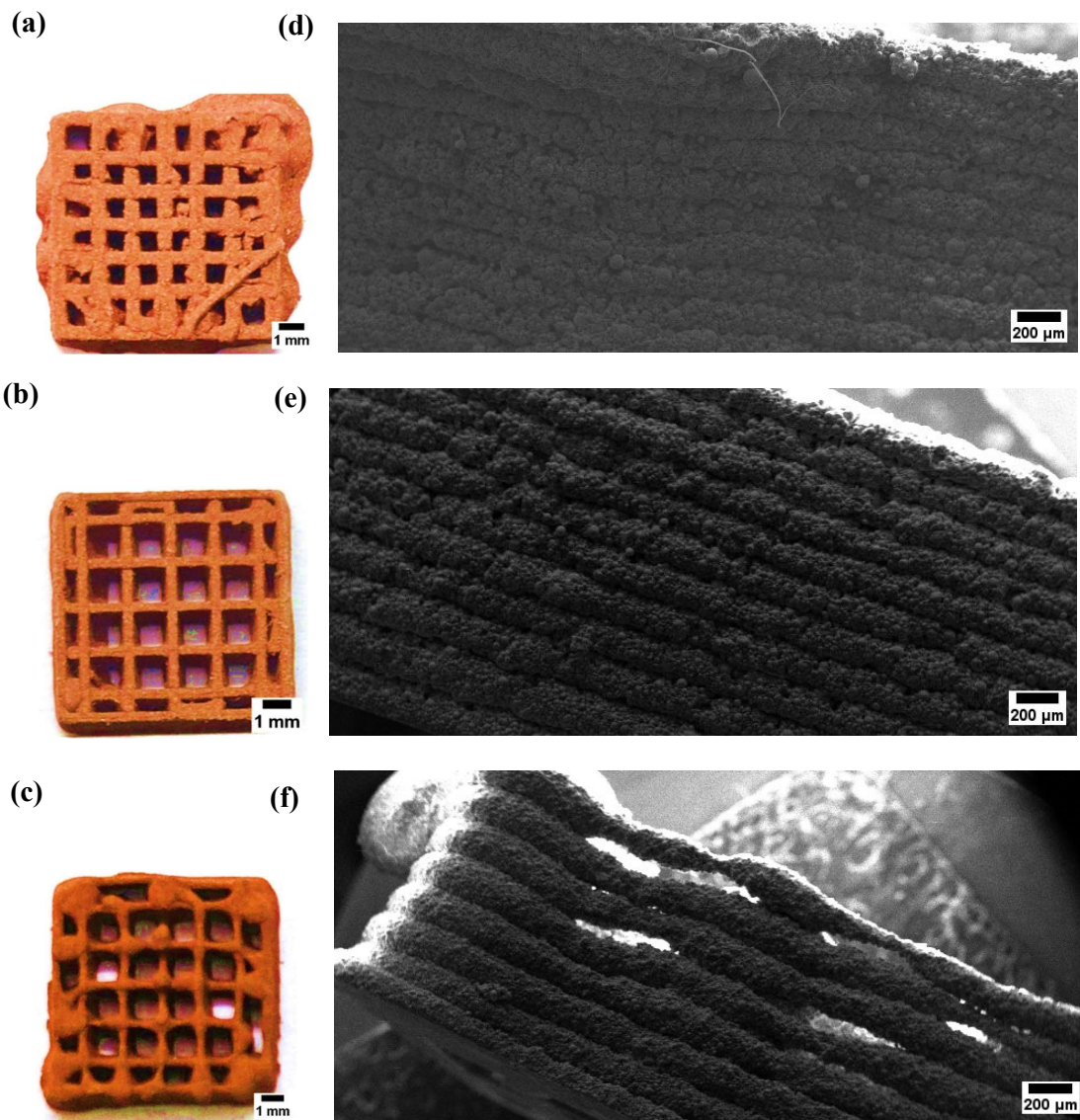


Fig. 5.3: Green *Cu* samples printed using layer height a) 60%; b) 70 % and c) 80 % and SEM images of the cross-section of green *Cu* samples printed using layer height d) 60%; e) 70 % and f) 80 %

As in the present work, the layer thickness is dependent on the size of the nozzle diameter with the values chosen as 60 %, 70 % and 80 % respectively of the corresponding nozzle diameter. Moreover, amongst the selected layer thickness values, 70 % of the nozzle diameter was found to give minimum dimensional deviation. To explain this combined effect of nozzle diameter and layer height, three samples with a layer height of 60%, 70% and 80% of a constant nozzle diameter were fabricated and the same are shown in Fig. 5.3. Fig. 5.3 shows the SEM images of the 3D printed samples at different layer height. It can be observed from Fig. 5.3 that with the change in layer height values, the shape of the deposited filament changed significantly. For 60 % layer height, some amount of squeezing was observed. Moreover, curved shape structures were observed in the case of samples fabricated using 80% layer height. A perfect structure was obtained for a 70 % layer height case. To explain this phenomenon, a schematic has been shown in Fig. 5.4.

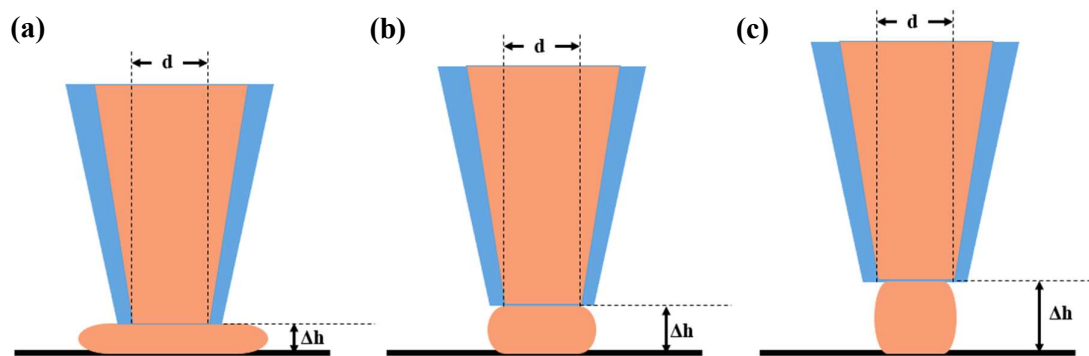


Fig. 5.4 Schematic of the DIW process with variation in the layer height. a) $\Delta h \ll d$ b) $\Delta h < d$ c) $\Delta h \leq d$ where Δh is the layer height and d is the nozzle diameter

It could be observed that when the layer height Δh was significantly lower than the nozzle diameter d , the *Cu* ink after extrusion through the nozzle will not be able dispersed instantly resulting in a deformed and squashed filament. Moreover, if the value of Δh is progressively increased to 70 % but still smaller than the nozzle diameter d , a uniform shape is achieved after the extrusion of the copper ink. This behavior can be attributed to the formation of an

optimal gap between the nozzle and the substrate, which is critical for ensuring proper extrusion and uniform dispersion of the ink during the DIW process. When the layer height (Δh) approaches a value nearly equal to the nozzle diameter, the extruded ink tends to maintain a cylindrical geometry as it is deposited.

This cylindrical shape is a result of the ink flowing in a confined, consistent manner without excessive spreading or deformation. However, during subsequent layer deposition, a change in the relative distance between the nozzle tip and the previously deposited layer can occur. This change is primarily due to the shrinkage of the earlier layer caused by solvent evaporation, which leads to a reduction in the actual height of the printed structure. As a result, the effective gap between the nozzle and the underlying surface increases, potentially affecting the accuracy and stability of the following layers. This underscores the importance of carefully optimizing the layer height relative to the nozzle diameter to maintain print fidelity and structural integrity throughout the entire deposition process.

5.1.1.3 Effect of print speed

The influence of varying print speeds on dimensional deviation during the DIW process was analysed in detail, and the findings are illustrated in Fig. 5.1. The results indicate that the maximum dimensional deviation occurred at a printing speed of 5 mm/s. This significant deviation can be attributed to the increased deposition of ink at localized spots due to the slower movement of the nozzle. At reduced print speeds, the ink has more time to accumulate in specific areas, leading to over-deposition and inconsistencies in layer thickness. This phenomenon is visually confirmed in Fig. 5.5 (a), where the green sample produced at a print speed of 5 mm/s exhibits thicker struts and a noticeably higher amount of accumulated material at various points. Such irregularities adversely affect the dimensional accuracy and overall quality of the printed structure.

As the printing speed was increased to 10 mm/s, a notable improvement in dimensional accuracy was observed. At this speed, the dimensional deviation was found to be at an optimum level. This improvement can be attributed to the balanced rate of material deposition and nozzle movement, ensuring consistent layer formation without excessive material buildup. The green sample corresponding to this printing speed, as shown in Fig. 5.5(b), demonstrates a highly accurate deposition pattern with appropriate stability and uniformity. The struts in the sample are well-defined, and there is no evidence of material accumulation, highlighting the effectiveness of this printing speed in achieving precise geometries.

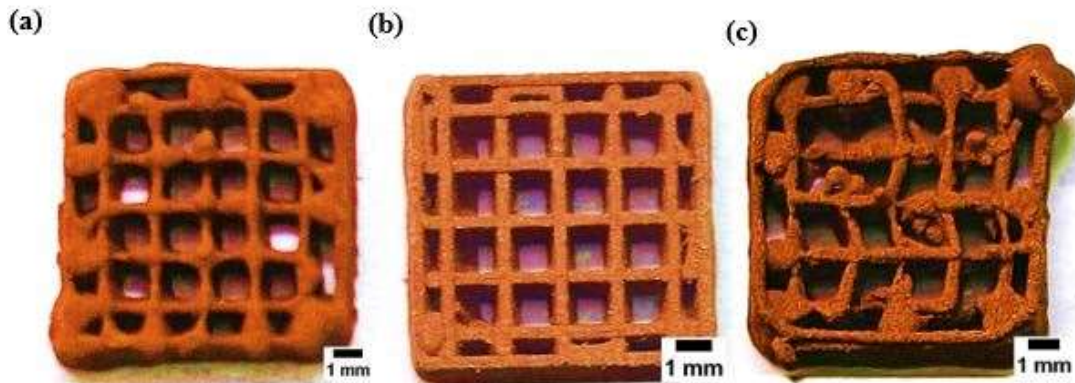


Fig. 5.5: Green HP-Cu samples fabricated using printing speeds of a) 5mm/s b) 10 mm/s and c)15mm/s

However, further increasing the printing speed beyond 10 mm/s resulted in an increase in dimensional deviation as evident from the image of the sample printed at 15 mm/s shown in Fig. 5.5 (c). Improper printing with the crumbling of the structure is obvious. Inappropriate extrusion and deposition of the *Cu* ink at such a high speed is the major cause of this effect.

At higher speeds, the nozzle movement is faster than the rate at which ink can be deposited and stabilizes effectively, leading to under-deposition or incomplete layer formation. This reduced interaction time between the nozzle and the substrate compromises the ability to

maintain accurate layer geometry, thereby increasing dimensional inaccuracies. The observed trends underscore the importance of selecting an appropriate printing speed to achieve optimal dimensional accuracy in the DIW process. A slower printing speed, while allowing for more material deposition, can lead to over-thickening and material accumulation, which adversely affects the printed structure. Conversely, excessively high printing speeds can cause under-deposition, resulting in poor layer adhesion and geometric inaccuracies. The printing speed of 10 mm/s represents a critical balance point where the deposition rate and nozzle movement are synchronized to produce precise and stable structures.

These findings are in agreement with the existing body of literature [48], which emphasizes the critical role of printing speed in controlling the quality and dimensional accuracy of DIW-fabricated components. By optimizing print speed in conjunction with other process parameters, it is possible to enhance the reliability and precision of the DIW technique, making it suitable for applications that demand high-quality and dimensionally accurate components.

5.1.2 Case Study

The present study aims to fabricate complex HP-*Cu* structures using DIW. The developed processing route has demonstrated the capability to successfully fabricate complex-shaped HP-*Cu* structures. The morphological analysis of the sintered HP-*Cu* samples, as presented in Fig. 5.6, reveals effective diffusion and strong interconnection between the copper particles, indicating successful sintering and particle bonding. However, the presence of micropores was also observed, which can be attributed to the decomposition and removal of the organic binder during the thermal treatment stage. These micropores, while

contributing to the overall porosity, may influence the mechanical and functional properties of the final structures.

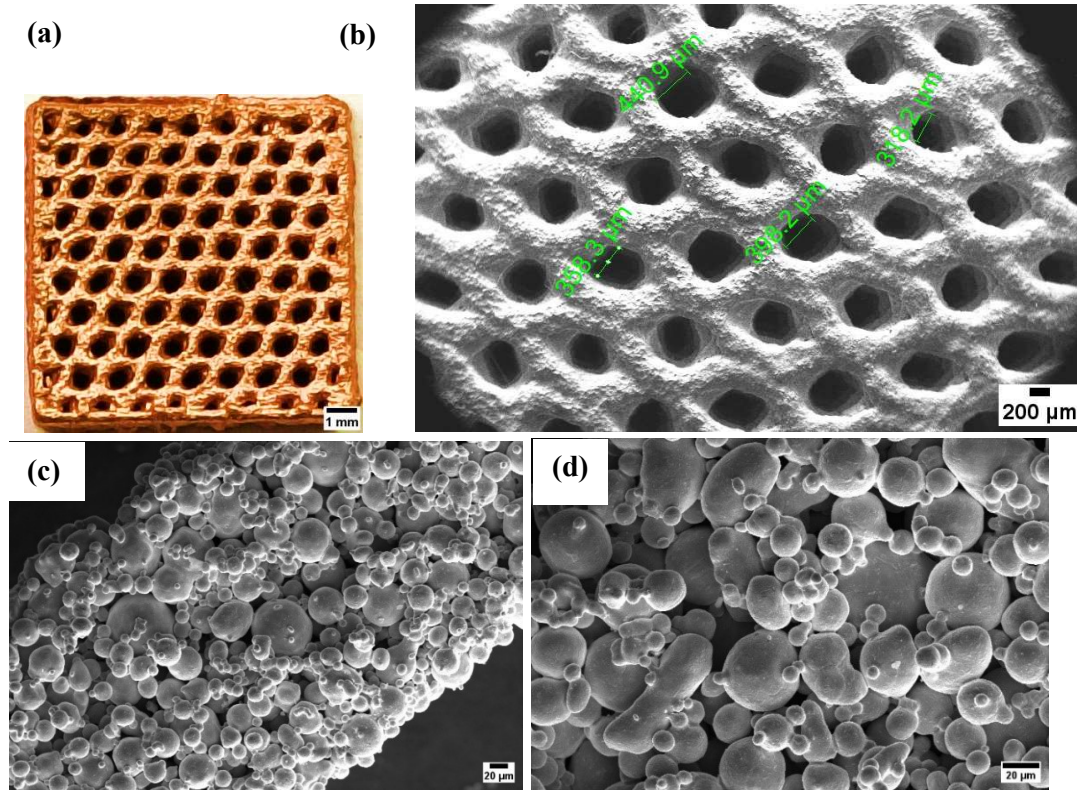


Fig. 5.6: a) Image of sintered honeycomb *Cu* sample fabricated using optimized printing parameters; b) SEM image of sintered sample, c) magnified view of strut (at 500 X) and d) SEM image (at 1000 X) showing interparticle bonding

Post-sintering measurements indicated a relative density of approximately 91%, suggesting a substantial degree of densification despite the inherent porosity. Furthermore, the hierarchical pore structure achieved in the final HP-*Cu* samples exhibited an average pore size of around 380 μm . This pore size, while indicative of successful formation of a porous network, also highlights the need for further refinement in processing conditions to tailor the pore architecture for specific energy storage or catalytic applications.

Moreover, to establish the effectiveness of the developed methodology, a thin-shaped *Cu* electrode sample of diameter 20 mm and with a pore size of 150 μm has been designed.

Such complex *Cu* structures are widely used in electrochemical energy storage applications such as lithium metal batteries. The sample has been fabricated using the optimized set of processing parameters for DIW as obtained from the analysis. From Fig. 5.7, it can be observed that the complex-shaped thin HP-*Cu* electrode sample was successfully fabricated using the developed methodology. From the analysis, the hierarchically controlled pore size fabricated sample was found to be $154 \pm 10 \mu\text{m}$.

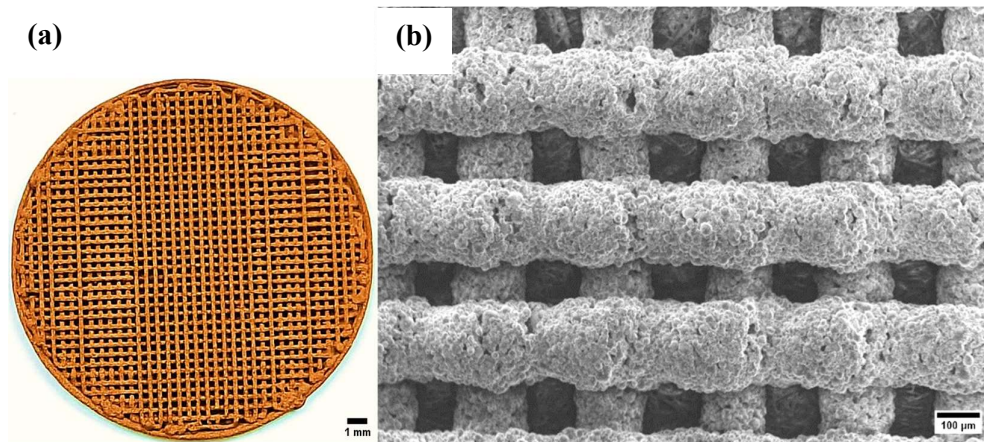


Fig. 5.7: (a) Porous *Cu* current collector green sample (b) SEM image of fabricated HP-*Cu* current collector

Moreover, a comparative study with the previously reported work related to the fabrication of HP-*Cu* has been performed and included in Table 5.3. It can be inferred from Table 5.3 that different works targeting the fabrication of HP-*Cu* samples have been reported. Almost all the previously reported works have used different AM techniques such as SLM, EBM and DIW. However, to date, none of the studies have reported the fabrication of HP-*Cu* samples with pore size of $150 \mu\text{m}$. The main difference in performance highlights the advantages of the HP- *Cu* structure, which was fabricated using the innovative methodology developed in the present study. The HP- *Cu* current collector, with its

hierarchical porous structure provides the higher surface area that reduces the dendrite growth.

Table 5.3- Comparison of ordered porous Copper structures produced by the additive manufacturing process

Sr. No.	Method used	Pore size (μm)	Compressive strength (MPa)	Relative density (%)	Application	Ref
1.	Direct Ink Writing	200	1.45	-	Lithium metal battery	[108]
2.	Powder bed Fusion	200	164	-	Spacecraft	[109]
3.	3D Printing	1000-2500	2.5-25	28-36	Thermal Management system	[110]
4.	Digital Light Processing	494.6	-	-	Fuel cells	[111]
5.	3D Printing	600	-	-	Battery	[112]
6.	Binder jetting	1000	-	-	Metallic Foam structures	[113]
7.	Electron Beam Melting	1000-2000			Heat Transfer	[114]
6.	Direct Ink Writing	154 \pm 10 μm	215	91	Energy storage device	Present study

The reason for achieving such a fine pore size in the sample could be attributed to the systematic optimization of DIW process parameters and the use of high particle loading 97 wt% Cu ink

While the present research demonstrates the successful fabrication of (HP-*Cu*) structures with pore sizes below 200 μm , certain limitations were observed that warrant further investigation. In particular, higher porosity in some samples could potentially compromise mechanical integrity and hinder optimal electrochemical performance. Additionally, a more uniform and finer pore size distribution is desirable to enhance surface area and improve the efficiency of energy storage applications. To address these issues, further refinement of the sintering parameters such as, temperature, duration, and atmosphere is essential.

This research represents a landmark contribution to the field of porous *Cu* current collectors for EES applications. By addressing the challenges associated with high particle loading in ink formulations and optimizing the DIW process, the study sets a benchmark for the fabrication of advanced materials tailored for energy storage technologies. The results demonstrate the potential of this approach to enable the scalable production of high-performance components, opening new avenues for innovation in the design of EES devices.

Hence, a further optimization study was conducted in this area with an expectation to attain a more controlled porosity and improved structural performance, which may open new horizons in tapping the potential of HP-*Cu* materials in high-performance energy storage systems and the same is reported in subsequent chapter.